A Software Environment for Studies of Precipitation Using Meteorological Radars and Satellites

Garcia, J.V.C.[1], Calheiros, R.V.[2], D' Oliveira, A. B.[3], Stephany, S.[4]

[1] *Programa de Pós-graduação em Computação Aplicada, Instituto Nacional de Pesquisas Espaciais (CAP/INPE), Brazil,* c4ll1b4n@gmail.com

[2] *Instituto de Pesquisas Meteorológicas, Universidade Estadual Paulista (IPMet/UNESP), Brazil,* calheiros@ipmet.unesp.br

[3] *Divisão de Satélites e Sistemas Ambientais, Centro de Previsão de Tempo e Estudos Climáticos, Instituto Nacional de Pesquisas Espaciais (DSA/CPTEC/INPE), Brazil,* augusto.oliveira@cptec.inpe.br

[4] *Laboratório Associado de Computação e Matemática Aplicada, Instituto Nacional de Pesquisas Espaciais (LAC/INPE), Brazil,* stephan@lac.inpe.br

(Dated: 18 January 2010)

1. Introduction

The synergistic use of different sensors for the observation of precipitation is an approach of growing importance, worldwidely. In particular, the combination of weather radar and environmental satellite data is used in many important applications, e.g. hydrological management and agricultural practices. The understanding of the correlation of precipitating structures observed in both images allows to validate forecasts based only on satellites images when radars are not available.In Brazil, multi-purpose observation of precipitation dates back to 1974, when a C-band non-coherent weather radar started operations at Bauru (lat 22°21'30" S, long 49°1'42" W) , in the central area of the State of São Paulo. In 1992 a S-band Doppler system (thereon BRU) substituted for the old C-band, enhancing substantially the potential for applications, in addition to broadening the research perspectives, mainly those focused on precipitation. In 1994, a second radar was installed in the West, at Presidente Prudente (lat 22°10'30" S, long 51°22'30") in network with the Bauru radar, largely increasing the area covered by radar in the state and adjacent regions. Both radars have recently undergone a substantial upgrade/update which significantly improved the quality of the rainfall measurements. BRU, in special, covers one of the most socio-economically important regions of the country, providing crucial support to Civil Defence and being extensively explored by the productive sector. Economic constraints preventing the deployment of a denser radar network led to the use of BRU to the outer radar ranges. The degradation of radar observation at those ranges prompted the developments of procedures to use satellite data jointly with the radar. Calheiros and D'Oliveira (2007) proposed a methodology to complement the far range radar observations with satellite radiometric data, in an attempt to extend the useful range of the radar.

A major challenge faced by the authors was to deal with images from different instruments. The task is made difficult by the form of presentation of these images. In order to perform comparative studies, on a pixel-to-pixel basis, it is necessary to correct for effects due to rotation and differences in resolution, besides the particular geometric distortions of each image. Many advances have been achieved in this field. There are several methods which take into account image rotation, as well as resolution discrepancy, but most of them do not contemplate the effects due to geometrical distortion (Gonzalez & Woods, 2007, and Jain, 1989). In their above mentioned work, Calheiros & d'Oliveira (2007) presented a technique to deal with this problem, taking into consideration the geometrical distortion of the image with lower resolution and employed an adaptative asymmetric (elliptic) Gaussian filter . In that particular study, the satellite image had a resolution more than 20 times lower than the resolution of the radar image. Also, the geometrical distortion of the radar image could be considered as negligible. The present paper introduces a new software environment which can be applied to an operational setting and, in a way, embeds a generalization of the technique presented in Calheiros and D'Oliveira (2007), by taking in account effects of geometrical distortion present in both images.This software is released under a GPL-2 license and is intended to quickly perform the comparative analysis of radar and satellite images for many precipitation events at a time. Notwithstanding, its is ready for application to other types of images, as exemplified later in this paper.

2. Material and Methods

In the following discussion the higher resolution image will be referred to as the *Source Image,* its post-processed image as the *Object Image* and the lower resolution image as the *Model Image*. The technique described in this work aims at reducing the resolution of the Source Image to the same resolution of the Model Image, creating in this process the Object Image. Besides this, the area in the real world, represented by its corresponding pixel in the Object Image should be as close as possible to the area represented by the corresponding pixel in the Model Image; in short, they should have similar geometric

distortions. The resolution of an image is degraded by means of a method like the Nearest Neighbor, or bicubic, being the pixels considered as points, i.e. with no real dimension. As a result, the Object Image generated by this process does not consider the geometric distortions of the Source Image and the Model Image. A comparative pixelwise study between the Object Image and the Model Image shows a high discrepancy, since corresponding pixels would be representing different areas in the real world (Jain, 1989 e Jensen & Lulla, 1987).

2.1 Non-linearly variable Elliptic Gaussian filter

In order to perform a remapping of the Source Image, in such a way that its geometric distortion and resolution become equivalent to the Model Image, Calheiros & d'Oliveira (2007) suggest the use of a filter to smooth the image in a non uniform way, before reducing its resolution as shown in Equation 1.

$$Filter_{i,j}(x,y) = \frac{\exp\left(-\left(\frac{x-(a_i/2)}{2}\right)^2 - \left(\frac{y-(b_j/2)}{2}\right)^2\right)}{\sum_{w=0}^{a_i}\sum_{z=0}^{b_j}\left(Filter_{i,j}(w,z)\right)} \tag{1}$$

The value for each pixel will depend on the value of its neighboring pixels (Gonzalez & Woods, 2007). It is assumed that this impact is suitably represented by a Gaussian distribution. In this sense Calheiros and D'Oliveira (2007) applied an Elliptic Gaussian filter on the Source Image, with a variation from pixel-to-pixel to take into account the heterogeneities of resolution and also geometric distortions. The objective of this filter is to smooth out the Source Image introducing a new geometric distortion equivalent to the Model Image one. The filter is expressed by Equation 1, where (x,y) represents the *x-th and y-th* pixel of the Source Image, a_x is the size of the filter along the x axis and a_y is the size of the filter along the y axis. Both a_x and a_y are calculated so that the Source and Model Images are matched, as illustrated in Figure 1. After applying the filter to all pixels of the Source Image, the resulting Objet Image is not only smoothed, since its resolution is degraded to the resolution of the Model Image, but also features similar geometric distortions.
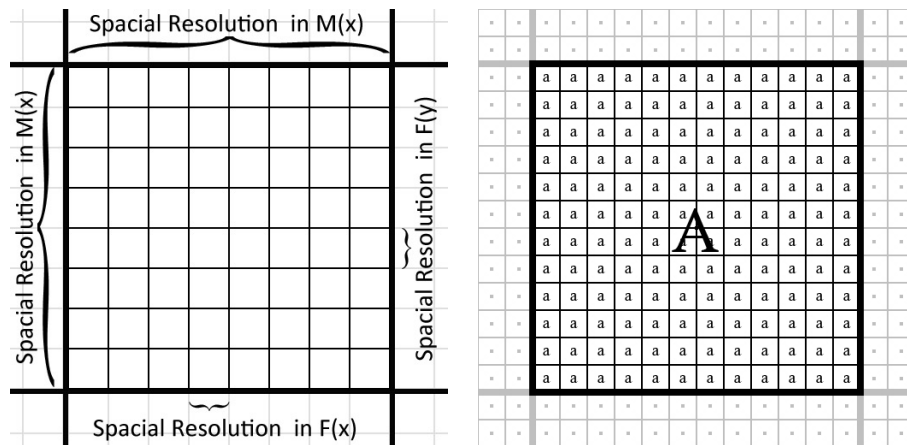

Fig. 1 – Left: Pixel sizes for the Source and Model Images. Right: Association of a pixel of the Model Image with pixels of the Source Image.

2.2 Remapping

The remapping of the Source Image into the Object Image is done using the nearest neighbor method. For each pixel in the Source Image it is associated the pixel in the Model Image with center coordinates closest to those of the Source Image pixel. Thus, each pixel in the Model Image corresponds to a set o pixels in the Source Image. The average value of those corresponding pixels in the Source Image is then computed, generating the resulting pixel in the Object Image. This procedure allows to generate an Object Image comparable in resolution and geometric distortion to the original Model Image. The geometry of the procedure is sketched in Figure 2.

3. Results and Discussions

3.1 Validation of the method

The validation of the present method is performed here by quantitatively evaluating the Object Image vis-à-vis the Model Image for the different methods used to obtain the Model Image - Object Image pairs. The statistical parameters P1, P4, P5 and P6 from Mecklenburg et al (2000) were used for evaluating each method. P1 is the distance between the centers of mass, P4 is the ratio of the medians, P5 is the ratio of the differences between the 25th and the 75th quartiles for both images, and P6 is the correlation between the images. Optimal agreement values are, then, zero (length unities), 100%, 100% and 1, respectively. Two sets of images were selected to test the method. The first is a single pair constituted by a sample 3D image generated by Computer Graphics – the Source Image – and the corresponding Model Image, which is a slightly distorted and lower resolution image from the Source Image. The second is a set of 8 pairs of images from different meteorological events. Each pair is composed of an image from a S-band weather radar, representing the Source Image, and the corresponding NOAA-18 satellite microwave image characterized later in the paper, playing the role of the Model Image (Calheiros and D´Oliveira, 2007).

Fig. 2 – Original 3D Source Image with good resolution and without distortion.

3.2 Application to a 3D Image

In order to evaluate the performance of the proposed method, the Computer Graphics 3D Source Image shown in Figure 2 was chosen to generate Object Images employing (i) the Calheiros & D'Oliveira method, (ii) weighted remapping without filtering, (iii) degradation of the resolution by the nearest neighbor procedure, (iv) bicubic degradation of resolution, and (v) bilinear degradation of resolution. These images are shown in Figure 3, that also includes the Model Image.

As can be seen in Table 1, the technique presented in Calheiros & D'Oliveira (2007) provided the best results for the four statistical parameters of Mecklenburg et al (2000). This demonstrates that the geometric distortion of the images has large impact on the quality of the image obtained by a method that degrades resolution. The bicubic method provided an Object Image with acceptable quality, followed by the bilinear method, being their performance affected by the geometric distortion of the images. However, they are faster than the method of Calheiros & D'Oliveira (2007), and should be considered in situations where image quality is not as relevant as processing time. The weighted remapping (that does not include the Gaussian filter) reached a poorer, yet acceptable result. The worst result was obtained by the nearest neighbour method. It is important to note that the weighted remapping and the nearest neighbor method are very similar, and are computationally the less costly of those considered in this work.
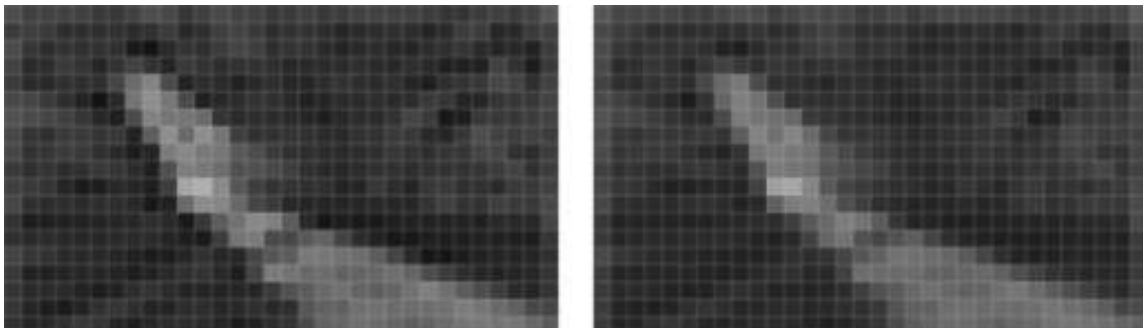
Fig. 3: Images corresponding to the 3D Source Image (from top to bottom and from left to right): Model Image and Object Images yield by the (i) Calheiros & d'Oliveira, (ii) weighted remapping,(iii) nearest neighbor,(iv) bicubic, and (v) bilinear methods.

Table 1 –Comparison of results for the Figure-3 Object Images generated by the different methods.

Method	P1	P4	P5	P6
Calheiros & D'Oliveira	0.013248	87.18125	91.10800	0.97420
Weighted Remapping	0.186221	42.41018	93.11111	0.75539
Nearest Neighbour	2.323841	22.54060	45.02028	0.56262
Bicubic	0.782121	74.41018	84.12097	0.81096
Bilinear	1.842132	51.42065	48.70101	0.74017

3.2 Application to a meteorological satellite image

   The use of satellite imagery to extend the useful range of a weather radar was the motivation for the work of Calheiros and D´Oliveira (2007). In that work, they employed pairs of corresponding radar and satellite images related to 8 different typical

precipitation events. The synergistic utilization of data from sensors of such different nature is the central issue of this paper, i.e. comparing images with different resolutions and geometric distortions. Here, satellite and radar images related to a particular precipitation event occurred at 01:31 GMT on March 16th, 2007 are considered. The radar CAPPI image (Source Image) has a 480 x 480 pixel resolution. Each pixel corresponds to approximately 1 km^2 at the Earth surface and its value expresses the reflectivity in dBZ. The corresponding satellite image (Model Image) was obtained by the channel 5 (high microwave) of the MHS (Microwave Humidity Sensor) instrument of the NOAA-18 polar orbit satellite. Its resolution ranges from ~10 to 35 km in the cross-track direction and the pixel value expresses the brightness temperature calculated from the measured radiance. The satellite image that covers an area equivalent to the radar image has typically 26 x 26 pixels. These images are shown in Figure 4, both centered at the Bauru radar location. To perform the comparison of both images, the brightness temperature of the satellite image is converted to reflectivity through an appropriate Tb –Z relationship (Calheiros and D´Oliveira, 2007). The resulting image obtained by the Calheiros & D'Oliveira method (Object Image) is then shown in Figure 5.
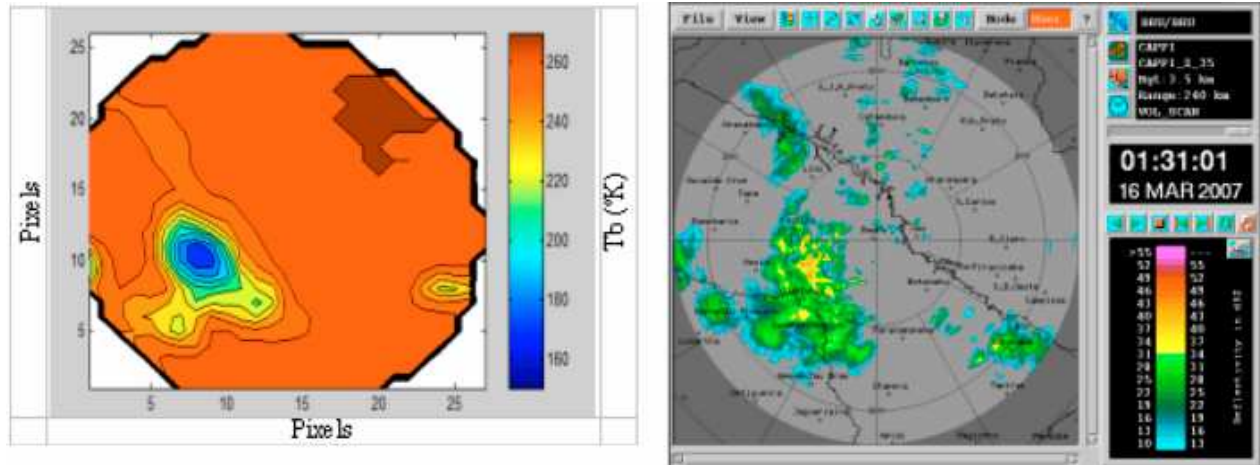

Fig. 4 – Left: Image of brightness temperature from Chanel 5 of MHS, NOAA18 satellite for the precipitation event occurred at 01:31 GMT on March 16th, 2007. Right: Image of the same event as observed by BRU

Table 2 shows the values of the statistical parameters of Mecklenburg et al. (2000) that were computed to check the quality of the processing performed on the images. Since the parameter P1 is measured in km, the distance between the centers of mass of the radar and the satellite images is less than 27 m. The parameters P4 and P5 have values close to 100%, implying that the variations of intensities in both images are comparable. The parameter P6 has also a good value, , indicating a high correlation between both images. It can be noted that the technique proposed by Calheiros & D'Oliveira provided and Object Image quite comparable to the Model Image.

Table 2 – Statistical parameters for the images shown in Figure 5.

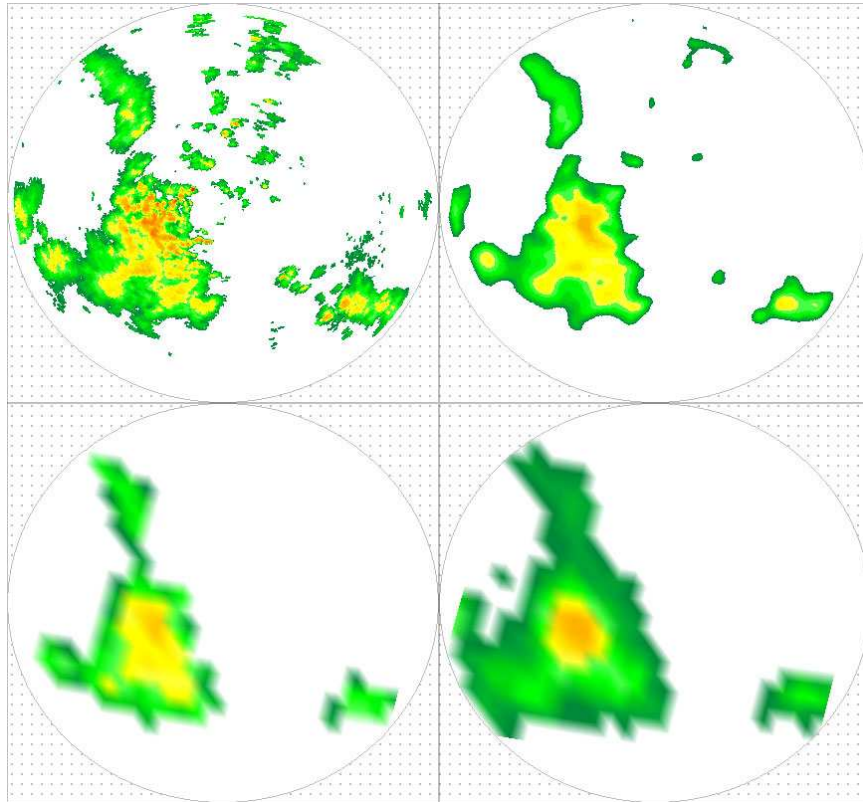| Variable	Obtained Value	Perfect Match
P1	0.026337	0.00
P4	89.452300	100.00
P5	131.966120	100.00
P6	0.817160	1.00

Fig. 5: Processed images for the precipitation event shown in Figure 4. Top left: Original non-filtered radar image (Source Image). Top right:Filtered-only radar image. Bottom left: filtered and remapped radar image (Object Image). Bottom right: satellite image (Model Image). The circle shown has radius of 240 km and it is centered at BRU.

4. Conclusions

The method proposed by Calheiros & d'Oliveira (2007) to degrade the resolution of Source Images taking into account the geometric distortion of the low-resolution Model Image obtained a better performance than the other four methods considered in this work for pixel to pixel comparison purposes. This method demands more processing time that the remaining methods tested here, but it is still very fast. This issue is currently being investigated. The developed software environment proved to be efficient for an operational scenario of weather forecasting and was successfully applied to a general sample radar-satellite image pair. The Calheiros & D'Oliveira method and the associated software will be employed soon in studies concerning the extension of the meteorological radar coverage, that are related to the nowcasting in the São Paulo Brazilian state.

References

Calheiros, R.V 1982:Meteorologia com Radar em São Paulo – Projeto RADASP/FAPESP.

Calheiros, R.V., D'Oliveira, A. B. 2007: Radar-satellite retrieval of cell structure: impact of Tb-Z relationships. In G*eophysical Research Abstracts*, **9**:10621.

Gonzalez, R.C. , Woods, R.E. 1987 Digital image fundamentals.

Jain, A. .1989: Fundamentals of digital image processing. Prentice-Hall, Inc. Upper Saddle River, NJ, USA.

Jensen, J Lulla, K. ,1987:Introductory digital image processing: a remote sensing perspective. *Geocarto International*, **2(1)**:65–65.

Mecklenburg, S. ; Joss, J. ; Schmid, W. Improving the nowcasting of precipitation in an Alpine region with an enhanced radar echo tracking algorithm, 2000: *Journal of Hydrology*, **239(1-4)**:46–68.